Neuron 51, 773–786, September 21, 2006 ©2006 Elsevier Inc. DOI 10.1016/j.neuron.2006.08.029

Clathrin-Mediated Endocytosis Is the Dominant Mechanism of Vesicle Retrieval at Hippocampal Synapses

Björn Granseth,[1,2] Benjamin Odermatt,[1,2] Stephen J. Royle,[1,3] and Leon Lagnado[1,*]
[1] MRC Laboratory of Molecular Biology
Hills Road
Cambridge, CB2 2QH
United Kingdom

Summary

The maintenance of synaptic transmission requires that vesicles be recycled after releasing neurotransmitter. Several modes of retrieval have been proposed to operate at small synaptic terminals of central neurons, including a fast "kiss-and-run" mechanism that releases neurotransmitter through a fusion pore. Using an improved fluorescent reporter comprising pHluorin fused to synaptophysin, we find that only a slow mode of endocytosis (τ = 15 s) operates at hippocampal synapses when vesicle fusion is triggered by a single nerve impulse or short burst. This retrieval mechanism is blocked by overexpression of the C-terminal fragment of AP180 or by knockdown of clathrin using RNAi, and it is associated with the movement of clathrin and vesicle proteins out of the synapse. These results indicate that clathrin-mediated endocytosis is the major, if not exclusive, mechanism of vesicle retrieval after physiological stimuli.

Introduction

Neurons transmit information at chemical synapses by the release of neurotransmitter contained within small vesicles (Katz, 1969). A synaptic terminal in the brain typically contains only 100–200 of these vesicles, so their fusion with the cell surface must be followed by efficient retrieval to maintain synaptic communication during ongoing activity. These endocytic mechanisms remain controversial, despite intensive study (Marte, 2002; Rizzoli and Betz, 2003; Royle and Lagnado, 2003; Tyler and Murthy, 2004; Dickman et al., 2005; Li et al., 2005).

Results from optical techniques applied to hippocampal neurons in culture have been interpreted as indicating that both fast and slow modes of endocytosis occur at synaptic boutons, although the molecular basis of these processes remain to be identified (Klingauf et al., 1998; Gandhi and Stevens, 2003). It is established that synaptic vesicles can collapse on fusion (Heuser and Reese, 1973; Li and Murthy, 2001; Zenisek et al., 2002; Llobet et al., 2003) and the machinery for retrieving this collapsed membrane by clathrin-mediated endocytosis (CME) is enriched at hippocampal boutons (Takei et al., 1996). What is less clear is the speed at which CME operates at small central synapses and its importance compared to other mechanisms of vesicle retrieval. In fact, it has been suggested that the large majority of vesicles released by physiological stimulation are recycled by a second, faster mechanism called "kiss-and-run," which operates in 1 s or less (Aravanis et al., 2003b; Harata et al., 2006). A key feature of the kiss-and-run model is that the vesicle is retrieved at the site of fusion *before* it has collapsed into the surface membrane (Fesce et al., 1994; Klyachko and Jackson, 2002; Aravanis et al., 2003b; Gandhi and Stevens, 2003; Richards et al., 2005). The strongest evidence for this mode of recycling derives from experiments investigating the behavior of single vesicles, either by observing the loss of a membrane dye from the synaptic bouton (Aravanis et al., 2003b; Richards et al., 2005) or by using synaptopHluorin, a fluorescent protein that reports fusion and retrieval of vesicles (Gandhi and Stevens, 2003). It is envisioned that neurotransmitter release during kiss-and-run occurs through a fusion pore less than 1 nm in diameter (Aravanis et al., 2003a).

The present study began with the aim of answering the following questions. Is slow retrieval of synaptic vesicles synonymous with CME? Does fast retrieval really reflect reversal of a transient connection through a fusion pore, or might it also be dependent on clathrin? And what is the relative importance of these different endocytic mechanisms during normal synaptic activity? To address these questions, we designed sypHy, a new and improved optical reporter of exocytosis and endocytosis made by fusing pH-sensitive GFP (Miesenbock et al., 1998) to the synaptic vesicle protein synaptophysin. We measured synaptic vesicle retrieval after single action potentials (APs), when fast kiss-and-run has been reported to be the predominant mode of fusion, but found only one mode of endocytosis, which occurred with a time constant of 15 s. Inhibiting CME completely blocked vesicle retrieval after weak stimuli. These results provide clear evidence against the idea that fast, clathrin-independent mechanisms of vesicle retrieval play a significant role at hippocampal synapses. We therefore conclude that CME is the physiological mechanism of vesicle retrieval.

Results

SynaptopHluorin Reported Only One Mode of Endocytosis

To monitor the fusion and retrieval of synaptic vesicles in response to weak stimuli, we began by using synaptopHluorin, a pH-sensitive GFP (superecliptic pHluorin) fused to synaptobrevin (Miesenbock et al., 1998; Sankaranarayanan and Ryan, 2000). We chose this technique because it is relatively direct: synaptopHluorin is quenched by the acidic pH inside a vesicle, but fluorescence emission increases when the interior of the vesicle connects with the external medium, and then rapidly declines again when the vesicle is retrieved and its interior reacidified. A second reason for using

*Correspondence: ll1@mrc-lmb.cam.ac.uk
[2] These authors contributed equally to this work.
[3] Present address: The Physiological Laboratory, School of Biomedical Sciences, Crown Street, University of Liverpool, Liverpool, L69 3BX, United Kingdom.

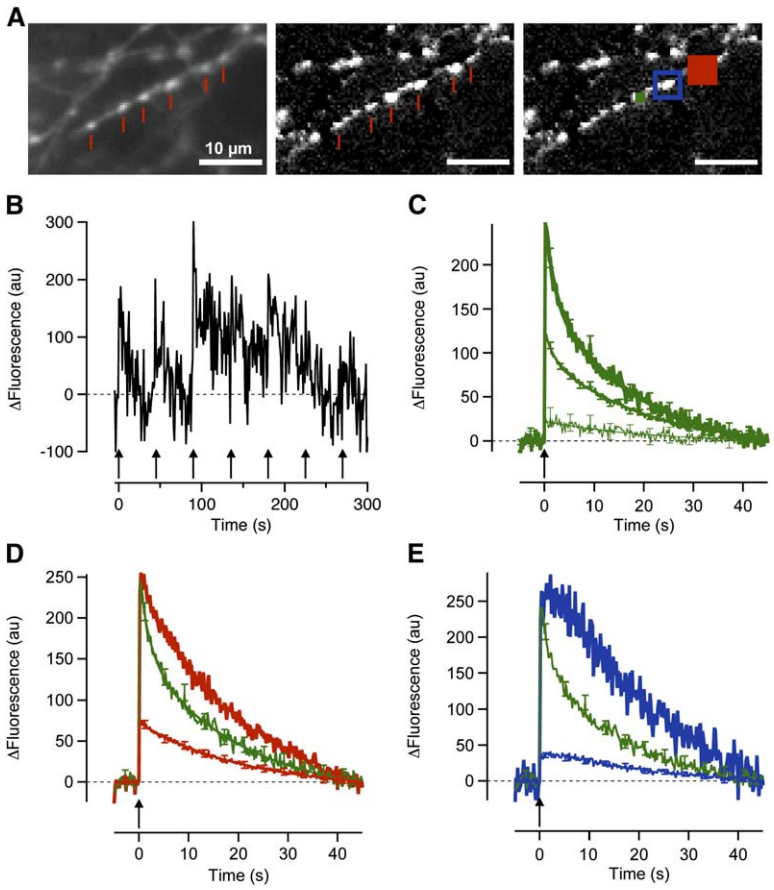

Figure 1. SynaptopHluorin Reported Only One Mode of Endocytosis

(A) (Left) SynaptopHluorin fluorescence at rest and (middle) a difference image showing the increase in fluorescence caused by 40 APs delivered at 20 Hz. The intensity changes were averaged over ROIs of different sizes, as shown to the right (green, 1.6 μm square; red, 4.8 μm square; blue, square perimeter with outer width of 4.8 μm and depth of 0.8 μm).

(B) Mean fluorescence change in a small ROI over one synapse, showing responses to single APs.

(C) Average synaptopHluorin responses to a single AP, measured using a small ROI. Bold trace was averaged from the 10% of synapses with the highest release probability (P_{rv}; n = 418 trials); recovery was biexponential with τ_{fast} = 2 s (36%) and τ_{slow} = 20 s. Thin trace was averaged from the 20% of synapses with the lowest P_{rv} (n = 742 trials); recovery was τ = 21 s. Trace of medium thickness was averaged from all synapses (n = 3897 trials); recovery was biexponential with τ_{fast} = 1.3 s (21%) and τ_{slow} = 20 s.

(D) Comparison of average synaptopHluorin signal triggered by a single AP in small (green) and large (red) ROIs, using the same synapses with the highest P_{rv}. Bold red trace is a scaled version to allow direct comparison of the kinetics of recovery and can be described by a single exponential with τ = 21 s.

(E) The synaptopHluorin signal averaged over a small ROI (green) compared with a surrounding area (blue), using the same synapses with the highest P_{rv}. The bold blue trace is a scaled version to allow direct comparison of the kinetics of recovery: it peaks and falls with a delay.

Error bars = SEM.

synaptopHluorin is that Gandhi and Stevens (2003) reported that this technique allowed the identification of three modes of endocytosis: kiss-and-run (<1 s), compensatory retrieval immediately following fusion (8–20 s), and a triggered mechanism that did not occur until the synapse was activated again. We attempted to repeat these observations, but instead we found that synaptopHluorin reported only one mode of endocytosis occurring with a time constant of 15 s.

An example of the synaptopHluorin signal triggered by a stimulus of 40 APs at 20 Hz is shown in Figure 1A and Movie S1 in the Supplemental Data. Two features are immediately obvious: the high background signal originating from synaptopHluorin on the cell surface, and its movement out of the synaptic bouton to neighboring regions of axons after exocytosis (Li and Murthy, 2001). The signal triggered by single APs is shown in Figure 1B, which is the mean intensity change over a square region of interest (ROI) of 1.6 × 1.6 μm centered over a single synapse, shown by the green square in Figure 1A. The size of this ROI was chosen to maximize the signal-to-noise ratio for detection of single fusion events, although visual inspection of the trace shows that the background noise made it difficult to select responses from failures. To extract the population behavior from this noise, we simply averaged the signals elicited by repeated trials, irrespective of whether or not an AP triggered release. The average time course of the response to a single AP, obtained from 3897 trials in 236 synapses, is shown by the trace of medium thickness in Figure 1C. The recovery phase could be described as the sum of two declining exponentials, with 21% of the fluorescence lost with τ_{fast} = 2 s, and the remainder with τ_{slow} = 20 s.

Did the fast decline in the synaptopHluorin signal reflect endocytosis or lateral movement of the reporter? To test the speed of movement, we compared the time course of the signal directly at the synapse with the surrounding region (blue outline in Figure 1A). Over the period that the fluorescence declined rapidly in the synapse, it rose in the neighboring axon (Figure 1E), demonstrating that synaptopHluorin was capable of leaving the synapse after fusion triggered by a single AP. To minimize the effects of movement on the signal we measured, the same set of experiments were reanalyzed using a larger ROI that also contained the axon either side of the synaptic bouton (4.8 × 4.8 μm). Within this larger area, recovery occurred in just one phase with τ = 21 s (Figures 1A and 1D). These results indicate that the slow decline in the synaptopHluorin signal at the synapse reflects endocytosis while the fast decline reflects outward movement of the reporter.

To increase the possibility of detecting a fast endocytic process, we made a separate analysis of synapses

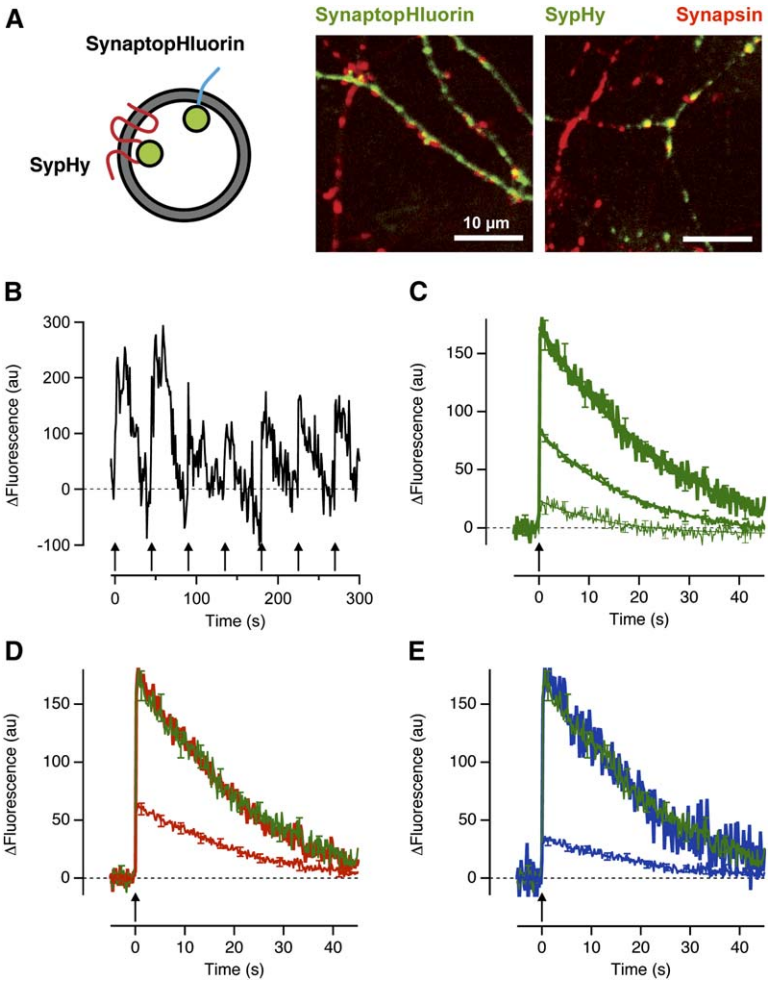

Figure 2. SypHy also Reported Only One Mode of Endocytosis

(A) (Left) Schematic illustration to compare the topology of sypHy and synaptopHluorin. Confocal images of neurons expressing (middle) synaptopHluorin or (right) sypHy, coimmunostained for synapsin (red).

(B) Mean fluorescence change in a small ROI over one synapse, showing responses to single APs. This synapse was of unusually high P_{rv}.

(C) Average sypHy signal triggered by a single AP, measured using a small ROI. The bold trace is averaged from the 10% of synapses with the highest P_{rv} (n = 330 trials); recovery was τ = 28 s. The thin trace is averaged from the 20% of synapses with the lowest P_{rv} (n = 636); recovery was τ = 16 s. The trace of medium thickness is averaged from all synapses (n = 2952); recovery was τ = 19 s.

(D) Comparison of average sypHy signal triggered by a single AP in small (green) and large (red) ROIs, using the same synapses of high P_{rv}. Bold red trace is a scaled version to allow direct comparison of the kinetics of recovery.

(E) SypHy signal averaged over a small ROI (green) compared with the surrounding area (blue). The bold blue trace is a scaled version. Error bars = SEM.

of low release probability, because these have been suggested to have the highest incidence of kiss-and-run (Gandhi and Stevens, 2003). The method we used to quantify release probability is described in detail below (Figure 4). We found that the synaptopHluorin signal in the 20% of synapses with the lowest release probability also declined monotonically after a single AP with τ = 21 s, which was indistinguishable from synapses of the highest release probability (Figure 1D, red trace).

SypHy, an Improved Reporter of Exocytosis and Endocytosis at the Synapse, also Measures Only One Mode of Endocytosis

To overcome the difficulties associated with the use of synaptopHluorin—high surface expression and diffusion out of the synapse—we designed a new reporter of exocytosis and endocytosis which is better localized to synaptic vesicles. This reporter used the same superecliptic pHluorin, but fused to the second intravesicular loop of synaptophysin and was named sypHy (Figure 2A; see also Y. Zhu, J. Xu, and C.F. Stevens, 2004, Soc. Neurosci., abstract). We suspected that sypHy might localize to synaptic vesicles better than synaptopHluorin because antibodies to synaptophysin provide excellent markers of synapses while barely staining the surface membrane (Valtorta et al., 2004). When overexpressed in hippocampal neurons, sypHy accumulated at synapses expressing synapsin and showed considerably less surface staining than synaptopHluorin (Figure 2A). This difference was quantified by measuring the fraction of total sypHy on the cell surface by dequenching all the protein in intracellular compartments using NH_4Cl (Sankaranarayanan and Ryan, 2000). Only 8% of sypHy was on the surface membrane, compared with 24% of synaptopHluorin. A detailed characterization of this and other properties of sypHy is provided in the Supplemental Data, where it is also shown that sypHy expression did not significantly alter the properties of exocytosis assayed using FM4-64.

The sypHy responses to single APs could be clearly detected at individual synapses, and the example in Figure 2B shows a series of responses from a synapse of high release probability. The improved signal compared with synaptopHluorin is also demonstrated in Movie S1. The sypHy fluorescence decayed with τ = 19 s. SypHy differed significantly from synaptopHluorin in the time course of the signal measured directly over the synaptic bouton using a small ROI: the response after one AP recovered monotonically and the fast phase of fluorescence loss was not observed, even in synapses of low release probability (Figure 2C). A second difference compared with synaptopHluorin was that the signal generated by sypHy appeared to remain localized to the bouton; there was no significant change in the

time course of recovery in a small ROI compared to a large one (Figure 2D), nor in the region directly over the synapse compared to the perimeter (Figure 2E).

SypHy and synaptopHluorin therefore provided very similar estimates of the rate of fluorescence quenching—about 20 s. A fast mode of endocytosis could not be detected with either pHluorin-based reporter. The sypHy and synaptopHluorin signals also recovered completely, which contradicts the idea that a proportion of vesicles released by a single AP remain stranded at the cell surface until the next stimulus arrives (Gandhi and Stevens, 2003).

Separating Vesicle Reacidification from Endocytosis

The direct cause of the decline in the pHluorin signal after exocytosis is reacidification of the synaptic vesicle by the action of the proton pump, which occurs only *after* vesicle scission from the surface membrane (Figure 3A). The decline in the pHluorin signal can be taken as a direct measure of endocytosis only if we assume that reacidification is instantaneous. The red trace in Figure 3B uses this assumption to describe the averaged sypHy response to a single AP as a single exponential. The time constant is 22 s and the fit is relatively good, except for a slight delay before the sypHy signal begins to decline.

A more accurate estimate of the rate of endocytosis can be obtained if the rate of vesicle reacidification is taken into account. Recent measurements using synaptopHluorin indicate that the time constant of reacidification (τ_r) is 3 to 4 s under the conditions of pH buffering we use (10 mM HEPES; Atluri and Ryan, 2006). We measured a similar time constant of reacidification using sypHy (Supplemental Data). This information allowed us to compare our measurements with a model in which quenching of sypHy fluorescence was controlled by two consecutive and irreversible reactions with first-order kinetics: endocytosis ($k_e = 1/\tau_e$) followed by reacidification ($k_r = 1/\tau_r$). The analytical solution to this model is shown in Figure 3A (van Santen and Niemantsverdiet, 1995) and the black trace in Figure 3B is a best fit with $\tau_r = 4$ s, which yields an estimate of $\tau_e = 15.5$ s. This two-step model also accounted for the slight delay before the sypHy signal began to recover and is likely to provide a more accurate estimate of the speed of endocytosis.

We also investigated the situation in which there are fast and slow modes of endocytosis. We used the predictions of Aravanis et al. (2003a) and Harata et al. (2006), who suggested that ~80% of vesicles released by a single AP are retrieved with a time constant of ~1 s. Figure 3B shows that these predictions do not agree with the time course of the sypHy signal. Our measurements with sypHy and synaptopHluorin are therefore most simply and accurately accounted for by a single mode of endocytosis with a time constant of 15 s.

An Estimate of the Average Time a Synaptic Vesicle Remains in Contact with the Cell Surface

The rate of vesicle reacidification that we measured with sypHy was obtained after a relatively strong stimulus of 40 AP at 20 Hz (Supplemental Data). Is it possible that reacidification after a single AP is much slower, perhaps becoming the rate-limiting process for the decline of pHluorin signals? We do not know of a mechanism by

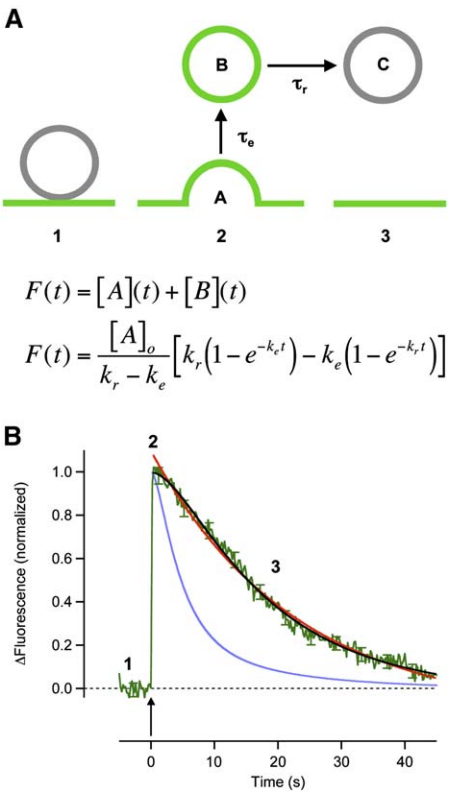

Figure 3. Separating Vesicle Reacidification from Endocytosis

(A) Schematic illustration of the processes that regulate the time course of signals obtained using intravesicular pHluorins. (1) The pHluorin is quenched in the acidic interior of the vesicle. (2) Fusion immediately causes the pHluorin to become fluorescent (state A), and it remains fluorescent after vesicle scission from the surface (state B). (3) The pHluorin is quenched as the vesicle interior becomes acidified (state C). The transitions A → B → C can be modeled as two consecutive reactions with first-order kinetics with time constants τ_e for endocytosis and τ_r for reacidification. The equations show the average time course of the fluorescence signal F at time t after vesicle fusion.

(B) A single exponential curve fit (red) with $\tau = 22$ s provided a relatively good description of the decay in sypHy fluorescence after a single AP measured within a large ROI (green). A better fit for the initial phase of the decay was obtained by the model in A (black) using a measured $\tau_r = 4$ s (Supplemental Data), yielding a $\tau_e = 16$ s. The light blue trace models the situation in which 80% of vesicles are taken up with $\tau_{e1} = 1$ s and the remainder with $\tau_{e2} = 16$ s, with both populations being reacidified with $\tau_r = 4$ s.

Error bars = SEM.

which this might occur, but we nonetheless set out to measure the rate of endocytosis using an approach that was independent of pH changes inside the retrieved vesicle. The method took advantage of the fact that while the vesicle lumen communicates with the outside, the pHluorin that it is carrying can be quenched by rapidly acidifying the medium, but after the vesicle is retrieved, changes in external pH do not affect its fluorescence (Merrifield et al., 2005; Atluri and Ryan, 2006). To make changes in external pH the only factor affecting pHluorin fluorescence, we applied bafilomycin A1, an inhibitor of the proton pump that blocks reacidification after endocytosis (Sankaranarayanan and Ryan, 2001).

The principle of the experiment is shown in Figure 4A. First, the fluorescence of sypHy on the surface of the

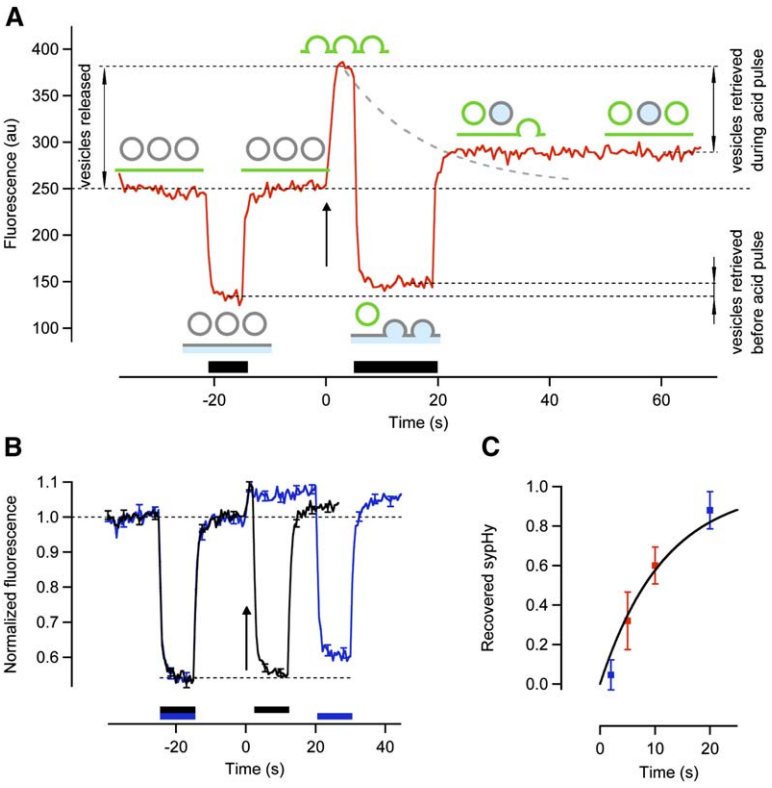

Figure 4. Monitoring Vesicle Contact with the Cell Surface by Rapidly Changing the External pH

(A) Average sypHy trace showing two periods of superfusion with pH 5.25, 20 seconds before and 2 seconds after 40 APs at 20 Hz (arrow). The schematic illustrations show the fluorescence (green) of three synaptic vesicles recaptured at different rates (from left to right: fast, medium, and slow) during various steps in the experimental protocol. To prevent vesicle reacidification after endocytosis, neurons were preincubated with the proton pump inhibitor bafilomycin A1. The first period of acidification (sky blue) quenches sypHy already on the cell surface. The second period also quenches sypHy inside fused vesicles yet to be retrieved. Note that vesicles retrieved during the period of acidification remain quenched. The fluorescence signal upon returning to physiological pH is that expected if all vesicles are retrieved with a time constant of 15 s (dashed grey line).

(B) Quenching vesicles released by a single AP. Acid was applied at delays of 2 s (black trace) or 20 s (blue). The AP was delivered at the arrow. After 2 s, 95% of the exocytosed sypHy is still on the surface and 59% was internalized during the subsequent 10 s of exposure to pH 5.25. After a 20 s delay, 88% of the sypHy was internalized and very little was endocytosed during the acid quench.

(C) The time course of sypHy retrieval after fusion triggered by a single AP. Blue points show sypHy internalized before the acid pulse, and the red points show the fraction internalized during application of acid. The black line is a best fit with a single exponential, yielding τ = 12 s.

Error bars = SEM.

bouton was quenched by switching the external medium from pH 7.4 to pH 5.25 and then back. A stimulus train of 40 AP at 20 Hz was then applied (arrow). The upward deflection synchronous with the stimulus is proportional to the amount of pHluorin in fused vesicles. Two seconds later, a second pulse of medium at pH 5.25 was applied to quench all sypHy fluorescence on the surface, including that originating from synaptic vesicles open to the external medium. The second application of acid did not reduce the fluorescence to the level observed before stimulation because some of the released vesicles were internalized before the acid was applied, and these remained fluorescent (reacidification having been blocked). Upon removing the acid, the fluorescence recovered to a steady level lower than that observed directly after stimulation. The lack of complete recovery was due to vesicles that were retrieved in the presence of acid and remained quenched. It was therefore possible to measure the proportion of released vesicles that were retrieved both before and during the acid pulse. The example in Figure 4A shows a 15 s application of acid beginning 2 s after the stimulus train has ended. The signal was consistent with endocytosis occurring with a time constant of 15 s after a train of 40 AP.

We applied the same approach to stimuli consisting of single APs (Figure 4B). In the first 2 s after fusion, only 5% ± 8% of the released sypHy was retrieved (black trace in Figure 4B). This measurement, taken on its own, would be consistent with an average time constant of endocytosis of about 40 s. Waiting 20 s before applying the acid pulse, we found that 88% ± 9% of vesicles had been retrieved (blue trace). By measuring the modulation of the fluorescence upon both adding acid and then removing it again, we assessed the proportion of vesicles retrieved at different times after the AP. This method provided an estimate of τ = 12 s for vesicle retrieval (Figure 4C), in close agreement with τ = 15 s measured using sypHy and synaptopHluorin as reporters of vesicle reacidification after endocytosis. Monitoring the connection of a fused vesicle with the surface of the cell by altering the external pH was only feasible with sypHy: using synaptopHluorin, the signal obtained upon applying acid was dominated by the quenching of fluorescence on the cell surface.

SypHy and SynaptopHluorin Report All Fusion Events

The results in Figures 1–4 contradict the suggestion that the predominant mode of endocytosis after weak stimulation operates in about 1 s (Aravanis et al., 2003b; Gandhi and Stevens, 2003; Harata et al., 2006). We wondered whether our inability to detect any fast endocytosis using pHluorin-based reporters might reflect a deficiency of the technique: is it possible that fast kiss-and-run events are being missed? A priori, one expects that the loss of protons from a vesicle will be at least as fast as loss of neurotransmitter or an FM dye. Nonetheless, we tested this point by measuring the fraction of vesicles in the readily releasable pool (RRP) that synaptopHluorin and sypHy report to be released after a single AP, allowing a comparison with the release probability measured electrophysiologically.

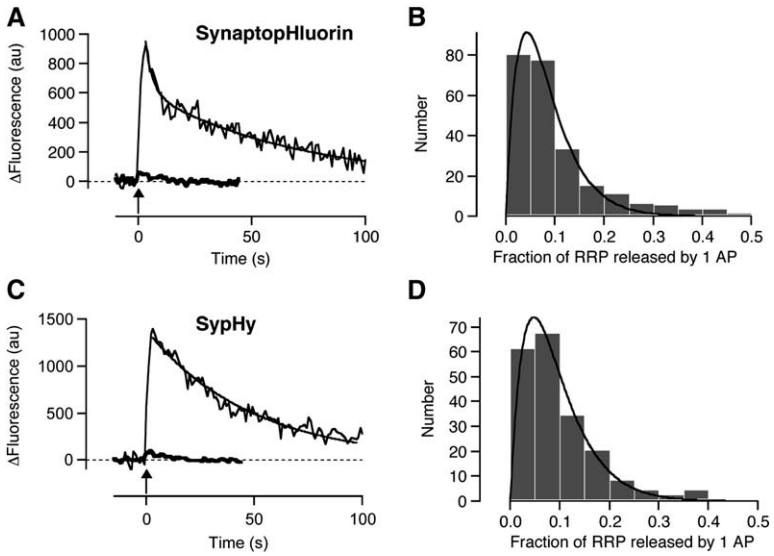

Figure 5. SynaptopHluorin and SypHy Reliably Reported Vesicle Release

(A) Average synaptopHluorin response of one synapse to a single AP (16 trials, bold trace) compared with the response of the same synapse to a train of 40 APs at 20 Hz (thin). Both were measured with a small ROI to best detect the signal immediately after fusion: the fast decline in the response to 40 APs was not observed with a larger ROI. The response to a single AP divided by the response to 40 APs measures the intrinsic release probability of vesicles in the RRP for this synapse.

(B) Histogram showing the distribution of intrinsic release probabilities over a population of 236 synapses in ten experiments. The mean value of P_{rv} was 0.089 ± 0.004, which would represent a synaptic release probability of 0.41 in a synapse with 4.6 vesicles in the RRP. Black line is a Gamma function with shape parameter α = 2.0 and rate parameter β = 24.5.

(C) Average sypHy response of one synapse to a single AP (17 trials, bold trace) compared with the response to a train of 40 APs at 20 Hz (thin).

(D) Histogram showing the distribution of P_{rv} in 201 synapses (17 experiments). The mean value was 0.095 ± 0.006. Black line is a Gamma function with shape parameter α = 2.0 and rate parameter β = 21.9.

SynaptopHluorin responses from a single bouton are shown in Figure 5A: the bold trace is the signal elicited by one AP, averaged from 16 trials, and the thin trace is the response of the same synapse to a single train of 40 APs delivered at 20 Hz. This stronger stimulus is sufficient to cause exocytosis of the whole of the RRP (Rosenmund and Stevens, 1996; Schikorski and Stevens, 2001; Rizzoli and Betz, 2005). By comparing the amplitudes of the responses, we estimated that a single AP released an average of 6% of the vesicles in the RRP at this synapse, providing a measure of the average intrinsic release probability of each vesicle in this population (P_{rv}). The variation in P_{rv} over 236 different synapses is illustrated by the histogram in Figure 5B, which could be described with a gamma function. The distribution of release probabilities measured electrophysiologically as vesicles released per synapse per AP is also a gamma function (Murthy et al., 1997). The mean fraction of the RRP released by a single AP was 0.089 ± 0.004 using synaptopHluorin and 0.095 ± 0.006 using sypHy (Figures 5B and 5D). These measurements represent a total release probability of 0.41–0.44 in synapses with an average of 4.6 docked vesicles per active zone (Rosenmund and Stevens, 1996; Schikorski and Stevens, 2001; Rizzoli and Betz, 2005). The average release probability reported by pHluorin was therefore slightly larger than the value of 0.35 measured electrophysiologically (Rosenmund and Stevens, 1996; Dobrunz and Stevens, 1997), indicating that pHluorin reliably records all fusion events and can therefore provide an unbiased view of the kinetics of endocytosis.

Endocytosis Occurred at a Constant Rate

Having measured the speed of endocytosis after a single AP, we wondered how it might be modulated by stronger stimuli. One model proposes that there is just one mechanism of retrieval in hippocampal synapses that is capable of retrieving a single vesicle at a maximum speed of 1 s^{-1}, but which gets progressively slower as more vesicles are released and the endocytic load increases (Sankaranarayanan and Ryan, 2000). We also found that the rate of endocytosis could be slowed, but only after particularly intense stimulation. For instance, Figure 8B shows that a train of 400 APs at 20 Hz was followed by recovery of the sypHy signal with a time constant of about 50 s. In comparison, the average firing rate of neurons in the CA3 region of the hippocampus is 1 Hz during performance of behavioral tasks, and high-frequency trains only occur in short bursts (Frerking et al., 2005). We therefore used sypHy to monitor endocytosis after delivering trains of 1 to 40 APs at 20 Hz, because these stimuli are more likely to emulate the physiological range of activities (Figures 6A and 6B). Regardless of how many vesicles within the RRP were released, the rate of fluorescence decay was almost fixed with a time constant that averaged 23 ± 1.5 s (Figure 6C). After correcting for the speed of vesicle acidification, we estimated that endocytosis occurs with τ = 17 s. These results indicate that the rate of endocytosis in hippocampal synapses is unlikely to be modulated during normal circuit activity.

Endocytosis Was Clathrin-Dependent

What is the mechanism that retrieves synaptic vesicles with a time constant of 15 s? The slow mode of endocytosis in retinal bipolar cells operates at a similar speed and has been shown to be dependent on clathrin and its accessory proteins (Jockusch et al., 2005). Is retrieval in hippocampal synapses also clathrin-dependent? To investigate this question, we inhibited CME using two different methods. The first was a dominant-negative approach entailing overexpression of the C-terminal

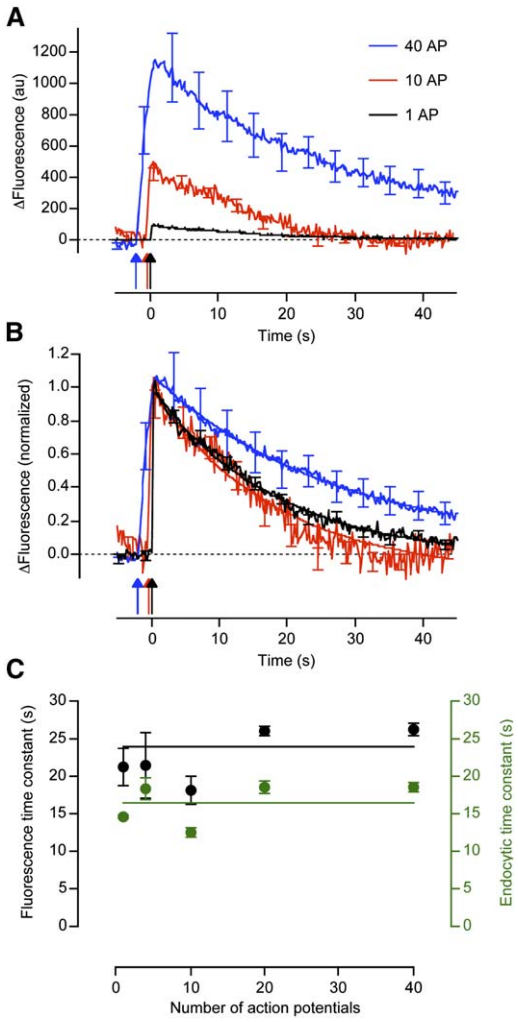

Figure 6. The Rate of Endocytosis Was Similar for a Range of Stimuli

(A) Average sypHy responses to 1 AP (black, n = 2236) and trains of 10 (red trace, n = 22) and 40 APs (blue trace, n = 24).

(B) Responses from (A) normalized to allow direct comparison of the kinetics of recovery.

(C) Time constant of sypHy fluorescence recovery (τ_f) for different numbers of APs at 20 Hz (black) and the corresponding estimates of endocytic time constants (τ_e) when reacidification time constant is 4 s (green). The solid horizontal lines indicates the average τ_f = 23 ± 1.5 s and τ_e = 17 ± 1.3 s. Each point comes from 21–151 synapses.

Error bars = SEM.

fragment of AP180—an accessory protein involved in CME (Ford et al., 2001). The second method was to deplete clathrin heavy chain (CHC) using RNA interference (Royle et al., 2005). Both these manipulations have been characterized as effective methods of inhibiting CME in cell lines without causing apoptosis or cell death (Ford et al., 2001; Motley et al., 2003; Royle et al., 2005).

Three days after transfection with siRNA against CHC, total clathrin levels were reduced to 12% ± 2% of that in controls, while scrambled siRNA had no significant effect (100% ± 9.8%; Figure 7A). This knockdown of clathrin effectively inhibited CME, assayed by the common approach of measuring the uptake of fluorescent transferrin: uptake was reduced by ~70% by depletion of CHC and by nearly 80% by overexpression of mRFP-AP180-C (Figures 7B–7D). Depletion of CHC and inhibition of transferrin uptake occurred in distal processes of the neuron as well as in the soma (Figures 7B and 7C). This inhibition of CME was not obviously detrimental to the health of neurons, because none of the cells took up trypan blue after these maneuvers (n = 20, 30, and 13 for Control, CHC RNAi, and mRFP-AP180-C, respectively). A more pertinent measure of the state of health of the neurons may be whether exocytosis was compromised by inhibition of CME: we found that the number of responding synapses over an area 203 × 203 μm was not significantly affected (12.5 ± 3.5, 14.5 ± 6.5, and 14.8 ± 4.3 for Control, CHC RNAi, and mRFP-AP180-C, respectively).

Inhibiting CME by either method completely blocked endocytosis of synaptic vesicles released by 4 APs at 20 Hz (Figure 7E). The simplest interpretation of this result is that all endocytosis after weak stimuli is clathrin-dependent. Retrieval was also substantially inhibited after the whole RRP was released by a train of 40 APs (Figure 7F). The partial recovery of fluorescence after this stronger stimulus might reflect incomplete block of CME under these conditions, or perhaps the appearance of a slower clathrin-independent process such as bulk retrieval, which is known to occur when the endocytic load is increased (Takei et al., 1996; Holt et al., 2004). Whatever the precise mechanism, the partial recovery after 40 AP was slow, so it cannot be taken as evidence for a fast clathrin-independent mechanism.

Endocytosis Was Associated with the Movement of Clathrin out of the Synapse

It has become increasingly clear that some proteins associated with synaptic vesicles can leak out of the synapse into the neighboring axon after fusion (Figure 1 and Movie S1; Li and Murthy, 2001; Wienisch and Klingauf, 2006; Fernandez-Alfonso et al., 2006). Where, then, does endocytosis occur—exclusively in the synaptic bouton, or also in the neighboring axon? Immunocytochemistry of hippocampal neurons in culture shows that clathrin, although concentrated at synapses, also distributes throughout neuronal processes, together with dynamin and adaptor and accessory proteins (Mundigl et al., 1998; Yao et al., 2003). A recent study monitoring the distribution of clathrin light chain A (LCa) fused to GFP found that very intense stimulation (750 APs at 20 Hz) caused a net movement of clathrin from the axon into the synapse of hippocampal neurons, although this did not begin until 14 s after the onset of stimulation, leading to the suggestion that there might first be a prolonged period of clathrin-independent endocytosis at the synaptic bouton (Mueller et al., 2004). Given the evidence that CME was the predominant mode of vesicle retrieval during normal levels of stimulation (Figures 1–7), we reinvestigated how the distribution of clathrin might change during synaptic activity. We used sypHy to identify sites of exocytosis and monitored synaptobrevin, synaptophysin, or LCa tagged with mRFP.

The difference images in Figure 8A provide examples of the changes in the distribution of these proteins caused by a stimulus of 40 APs at 20 Hz. The concentrations of mRFP-synaptobrevin and LCa-mRFP decreased immediately over the bouton while rising in

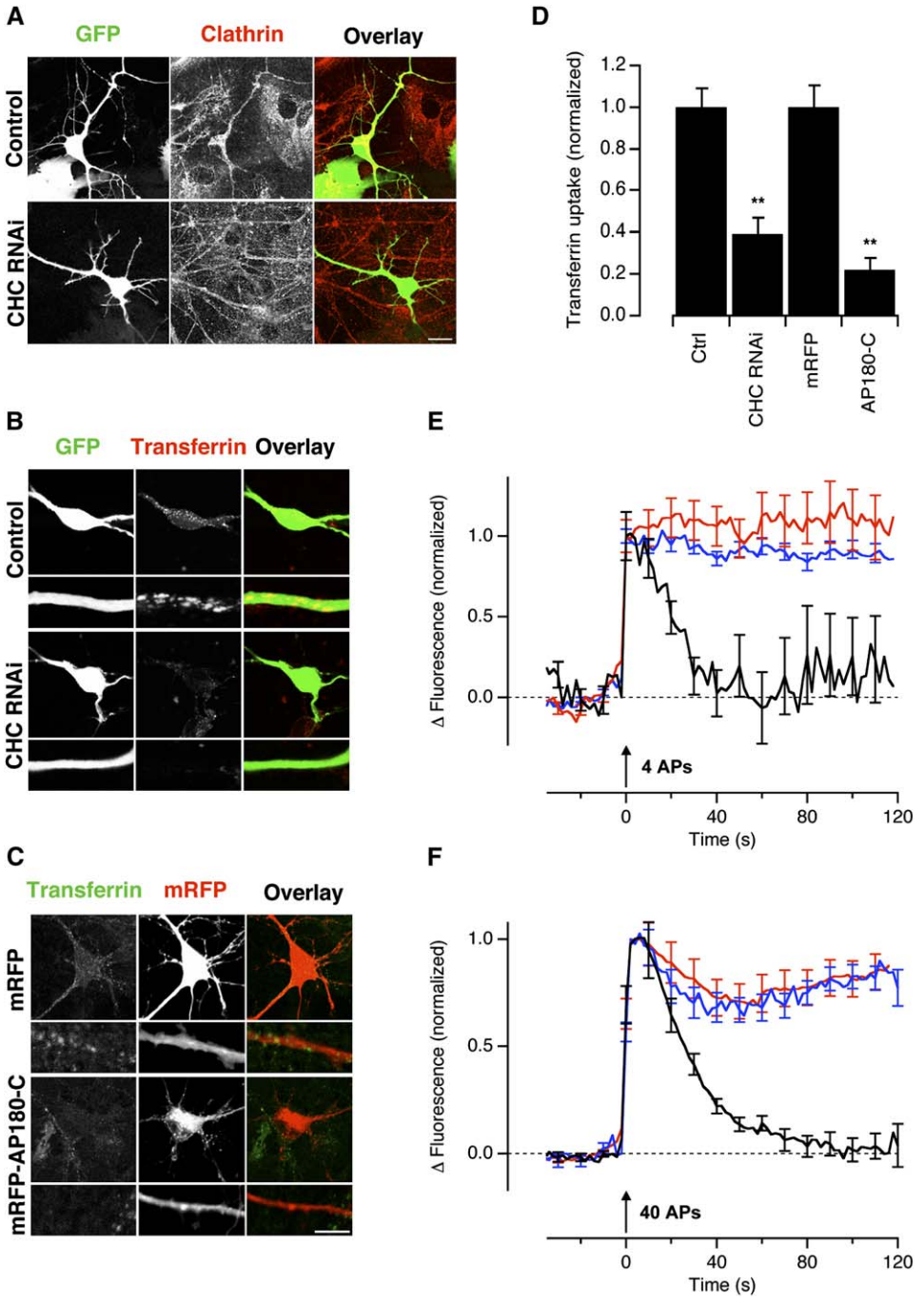

Figure 7. Inhibition of Clathrin-Mediated Endocytosis in Hippocampal Neurons Blocked Vesicle Retrieval after Weak Stimuli

(A) Depletion of CHC in hippocampal neurons by RNAi. Example images of neurons cotransfected with GFP (green) and either control or CHC siRNA. Cultures were fixed after 3 days and immunostained for CHC (red). Scale bar, 20 μm.

(B) Effect of CHC RNAi on CME assayed by transferrin uptake. Cells were cotransfected with GFP (green) and either control or CHC siRNA, then incubated with transferrin-Alexa546 (red). Examples are images of transferrin uptake at the soma (upper frame) and dendrites (lower frame).

(C) Effect of mRFP-AP180-C on CME. Cells were transfected with mRFP or mRFP-AP180-C (red), and then incubated with transferrin-Alexa488 (green). Scale bar, 5 μm (dendrite) and 20 μm (soma).

(D) Bar chart comparing transferrin uptake at the soma under these various conditions (n = 10–16).

(E–F) Inhibition of CME blocked vesicle retrieval after weak stimuli. Exocytosis was stimulated with either 4 (E) or 40 (F) APs at 20 Hz. Responses to 4 APs are from 130–303 synapses from five to nine experiments. Responses to 40 APs are from 107–204 synapses from four to eight experiments. Normalized fluorescence traces were recorded from cells transfected with sypHy and either CHC RNAi (blue) or mRFP-AP180-C (red). Control traces (black) are pooled from cells cotransfected with mRFP or with both mRFP and control siRNA.

Error bars = SEM.

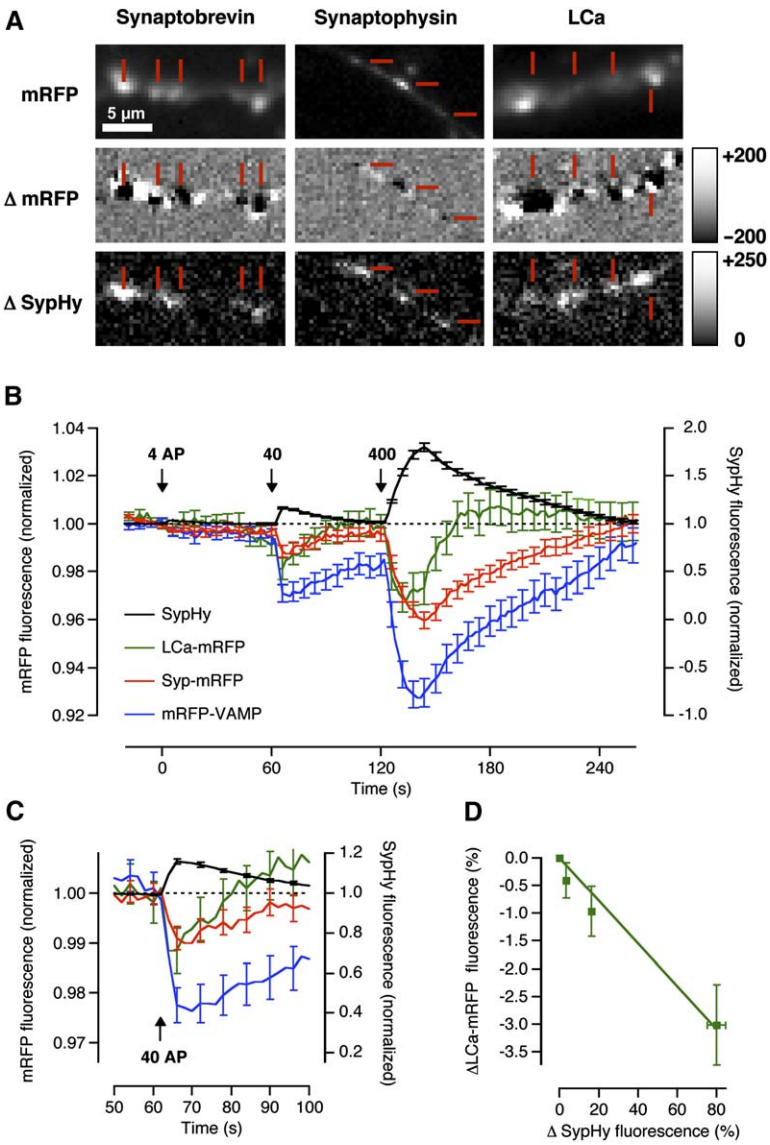

Figure 8. Clathrin, Synaptobrevin, and Synaptophysin Moved out of the Synapse upon Stimulation

(A) (Top) Example images obtained from neurons cotransfected with sypHy and either mRFP-synaptobrevin, synaptophysin-mRFP, or LCa-mRFP, together with (middle) a difference image showing the change in distribution caused by a train of 40 APs. (Below) Synapses were identified by sypHy responses. Note that synaptobrevin and clathrin leave the synapse and accumulate in neighboring regions. Red lines indicate sites of mRFP decrease; note the colocalization of these sites with exocytic zones.

(B) Average time course of the change in mRFP fluorescence in response to 4, 40, and 400 APs at 20 Hz, measured using an ROI of 1.2 × 1.2 μm. Each trace is averaged from five experiments (229–423 synapses). The sypHy response (black trace) is averaged from 62 synapses.

(C) Expansion of the response to 40 APs (from [B]) showing that the fall in the amount of clathrin at the synapse occurred within 2 s and recovered before synaptophysin or synaptobrevin.

(D) The fall in the amount of LCa-mRFP at the synapse was proportional to the amount of exocytosis, as judged from the peak amplitude of the sypHy signal. The line fitted to the points goes through the origin.

Error bars = SEM.

the adjacent axon, demonstrating net movement away from the active zone. The movement of synaptophysin-mRFP was harder to assess directly in these images because the levels of synaptophysin-mRFP or sypHy were low in cells expressing both synaptophysin-based constructs (Figure 8A). Therefore, to allow a quantitative comparison of the movements of synaptophysin-mRFP and mRFP-synaptobrevin, we measured the *relative* change in intensity of each protein in an ROI of 1.2 × 1.2 μm centered over each synapse (n = 230–423). Figures 8B and 8C show that the fall in the concentration of synaptophysin-mRFP at a synapse averaged less than half that of mRFP-synaptobrevin (mRFP-VAMP) after a train of 40 APs, confirming that synaptophysin was less mobile than synaptobrevin.

Two observations suggest that clathrin effectively "tracks" the vesicle proteins leaving the synapse. First, the amount of LCa-mRFP leaving the synapse was proportional to the number of vesicles released by the stimulus, as assessed by the amplitude of the sypHy signal (Figures 8B and 8D). Second, the movement of LCa-mRFP began without a significant delay and peaked with the sypHy signal (Figure 8C). The movement of clathrin out of the synapse together with synaptophysin and synaptobrevin is most easily explained as representing CME of vesicles at sites removed from the vesicle release site. This interpretation is consistent with studies showing that the machinery for CME is not at the active zone, but in the surrounding regions of membrane (Heuser and Reese, 1973; Ringstad et al., 1999).

Discussion

The kinetics of endocytosis at hippocampal synapses have been studied intensively for a number of years, but to our knowledge this is the first study to assign a molecular mechanism to a kinetically defined mode of retrieval. The results provide a relatively simple picture of vesicle recycling at hippocampal synapses: after physiological levels of activity, CME with a time constant of about 15 s retrieves all vesicles.

A basic feature of our results is that a fast mode of endocytosis could not be detected, even though it has been suggested that kiss-and-run operating in about 1 s predominates after weak stimuli (Aravanis et al., 2003b; Gandhi and Stevens, 2003; Harata et al., 2006). Our conclusions are based on a number of observations. Two reporters, sypHy and synaptopHluorin, only detected a slow mode of endocytosis with time constant of 15 s, even after release triggered by single APs. Further, two different methods of using pHluorins produced similar results: measurement of vesicle reacidification after retrieval (Figures 1–3) and measurements of the time for which a synaptic vesicle remains in contact with the cell surface by applying pulses of acid (Figure 4). The speed of endocytosis was the same at synapses of high and low release probability (Figures 1 and 2) and constant for a range of stimulus strengths (Figure 6). This kinetic evidence for a single mechanism of endocytosis was supported by the observation that two different methods of inhibiting CME blocked vesicle retrieval after weak stimuli: overexpression of a dominant-negative and knockdown of CHC using RNAi (Figure 7).

Two further observations indicated that vesicles collapsed upon fusion. First, exocytosis triggered by single APs was followed by loss of synaptopHluorin from the vesicle membrane into the surrounding axon (Figure 1), an observation which is difficult to explain on the basis of a connection through a proteinaceous fusion pore. Second, clathrin redistributed out of the synapse and then back again after releasing the whole RRP, also indicating movement of vesicle membrane proteins away from the site of fusion (Figure 8).

These results bring us to the conclusion that mechanisms of endocytosis that are fast and independent of clathrin, such as kiss-and-run, do not retrieve a significant fraction of synaptic vesicles at hippocampal boutons. We would not argue that the observations provide proof that kiss-and-run never occurs, but it is clear that such a mechanism does not need to be invoked to account for measurements obtained with sypHy and synaptopHluorin. In our judgment, these reporters provide signals that are more directly related to endocytosis than those obtained with FM dyes (Harata et al., 2006).

Analyzing SynaptopHluorin Signals

More complex signals from synaptopHluorin have been observed in a recent study of hippocampal synapses, and these were interpreted as reflecting three distinct modes of endocytosis, including a fast kiss-and-run mechanism occurring within 1 s (Gandhi and Stevens, 2003). We suspect that the disagreement with the present observations reflects two basic differences in methods of analysis.

(1) While Gandhi and Stevens (2003) began their assessment of the kinetics of endocytosis by selecting quantal responses out of the background noise, we simply averaged all traces, whether or not the AP triggered fusion. We found that selecting traces containing a response to an AP on statistical grounds introduced an intrinsic bias that causes "up-noise" to be included in the average (i.e. upward deflections in the trace unrelated to a true exocytic response). This up-noise appears as a fast transient in the synaptopHluorin signal that might be mistaken as a fast endocytic process, as described in the Supplemental Data. Our approach of averaging all records obtained after a single AP gives an accurate representation of the average behavior over a population of synapses while minimizing the possibility of bias introduced by a selection procedure.

(2) Gandhi and Stevens (2003) quantified the synaptopHluorin signals over an ROI 2.6 × 2.6 μm so as to maximize the signal-to-noise ratio for detection of quantal events. We found that diffusion of synaptopHluorin out of a small ROI caused a fast decline in the signal that was unrelated to endocytosis, and that a larger ROI was required to prevent significant diffusional loss of the reporter (Figure 1). The lower mobility of sypHy minimized this potential artifact (Figure 2).

Investigating Endocytosis with FM Dyes

The idea that fast kiss-and-run is the predominant mode of exocytosis during stimulation at low frequency has also been suggested on the basis of experiments in which exocytosis at hippocampal boutons is assayed by first loading a large number of vesicles with FM dyes that stain retrieved membranes, and then observing the kinetics of destaining upon stimulation (Klingauf et al., 1998; Pyle et al., 2000; Harata et al., 2006). It is argued that changes in the time course of destaining observed with dyes of different hydrophobicities and/or quenchers reflects a population of vesicles that fuse through a small and transient connection that limits the amount of dye lost by exocytosis. The conception of the situation used to interpret these signals is a vesicle immediately losing its dye directly into bulk solution (Figure 1B of Harata et al., 2006), but this neglects the fact that the dye is released into an environment where it can partition into membranes in which it will remain fluorescent. First there is the synaptic cleft, which is a narrow sandwich of membranes only 15 nm apart, spanned by large hydrophobic proteins (Schikorski and Stevens, 2001). Then there are the pre- and postsynaptic processes, which often run alongside each other for some distance in the en passant synapses formed in culture, as well as the layer of glial cell membranes along which these neuronal processes travel. An FM dye molecule leaving the vesicle will remain fluorescent as long as it partitions into any of these nearby membranes, and the signal will only be completely lost when all dye molecules have "escaped" this hydrophobic environment into the bulk solution.

To interpret the kinetics of FM destaining in terms of the behavior of the synaptic vesicle, it is therefore essential to identify the process that is rate-limiting. If the vesicle collapses, we expect that destaining will be rate-limited by diffusion out of the synaptic cleft and adjoining processes of the neurons, because these distances are much greater than the diameter of a vesicle (~40 nm). But what if a vesicle only releases dye through a putative fusion pore? This situation is harder to judge with the information available at present. The diffusion coefficient of FM1-43 in a single membrane is about 1 $\mu m^2 s^{-1}$ (Zenisek et al., 2002), but after leaving the vesicle, diffusion will be hindered by the large hydrophobic proteins that span the narrow space between adherent membranes of the pre- and postsynaptic neurons.

A second observation leading to the idea of kiss-and-run comes from experiments in which weak stimuli are

applied to trigger exocytosis at low rates; the amount of FM1-43 that is lost varies from event to event (Aravanis et al., 2003b), as does the speed of loss (Richards et al., 2005). The larger events have been attributed to full collapse of the vesicle and the smaller events to partial loss of the dye through a small fusion pore. But the amplitude of the signal originating from vesicle to vesicle is also expected to vary if they all collapse, because the size of vesicles varies. It is therefore important to have a good understanding of this source of variation before invoking different modes of exocytosis. The distribution of synaptic vesicle diameters observed in hippocampal neurons indicates that the volume of the largest 16% will be 2.4 times that of the smallest 16% (Harata et al., 2001). Further, the distribution of charge injected during evoked miniature excitatory postsynaptic currents in cultured hippocampal neurons is not a Gaussian distribution, but is strongly skewed towards larger events, which also indicates nonuniform vesicle sizes (Bekkers and Stevens, 1995; Franks et al., 2003). Does variability in unitary FM1-43 signals reflect this expected source, or must one invoke a kiss-and-run mechanism to obtain a reasonable explanation?

Perhaps the biggest difficulty with the idea that kiss-and-run is the normal mode of exocytosis during low-frequency stimulation is the lack of electrophysiological evidence to support it. A very large number of experiments indicate that neurotransmitter release from small vesicles is quantized, and Katz's hypothesis has been widely accepted to hold at central synapses as well as the neuromuscular junction (Bekkers, 1994; Auger and Marty, 2000). Indeed, a recent study demonstrates that the quantal size at hippocampal synapses does not vary with release probability (Biro et al., 2005). Electrophysiological measurements also demonstrate that fusion events involve release of a quantum of neurotransmitter with a time constant less than 100 μs (Stiles et al., 1996; Bruns et al., 2000), and such rapid and complete release of vesicle contents is generally thought to require rapid dilatation of the connection between the vesicle and the synaptic cleft. In contrast, it has been estimated that the radius of the fusion pore formed by small vesicles might be between 0.3 nm and 1 nm, through which glutamate is expected to be lost with a time constant between 1 and 6 ms (Klyachko and Jackson, 2002; Richards et al., 2005). The idea that hippocampal synapses usually release neurotransmitter in a low "whisper" through a narrow fusion pore currently lacks electrophysiological evidence to support it.

Fast and Slow Endocytosis at the Synapse

Do fast mechanisms of vesicle retrieval occur at other synapses? Perhaps the most direct method for measuring endocytosis is the capacitance technique, and a number of groups have applied this method to the large ribbon synapse of retinal bipolar cells. All find that there are fast and slow modes of endocytosis occurring with time constants of about 1–2 s and 10–15 s (Neves and Lagnado, 1999; Heidelberger et al., 2002; Hull and von Gersdorff, 2004). Stimuli just sufficient to deplete the RRP are followed almost exclusively by fast retrieval, but as the strength of stimulation is increased, the slow mechanism recycles an increasing proportion of the excess membrane (Neves and Lagnado, 1999). Experiments using peptides and protein domains targeting CME demonstrate that the slow mode of retrieval is clathrin-dependent, while the fast mode is clathrin-independent (Jockusch et al., 2005). But fast endocytosis in bipolar cells cannot be described as kiss-and-run. Interference reflection microscopy directly monitors expansion of the surface membrane and shows that brief stimuli cause all fused vesicles to collapse, and that this excess membrane is then retracted with a time constant of 1 s, reflecting fast endocytosis (Llobet et al., 2003). Also, total internal reflection fluorescence microscopy of individual vesicles labeled with FM1-43 shows that all detectable fusion events are followed by complete loss of the dye, indicating free exchange of lipid between the vesicle and cell surface after fusion (Zenisek et al., 2002).

In *Drosophila*, evidence that kiss-and-run occurs in animals with mutations in endophilin has recently been called into question (Verstreken et al., 2002; Dickman et al., 2005), while capacitance measurements at mossy fiber terminals in the hippocampus show that vesicles are retrieved in a mean time of 10 s (Hallermann et al., 2003). At the Calyx of Held, retrieval of single vesicles within 100 ms was initially reported (Sun et al., 2002), but a more recent study concludes that the rapid capacitance transient interpreted to be kiss-and-run was not related to transmitter release, and that all vesicles are recovered by a process with a time constant of 10 to 25 s (Yamashita et al., 2005). In the ribbon synapse of hair cells, all endocytosis triggered by depolarization occurs with time constants of 8–15 s, although a fast mechanism with a time constant of 300 ms can be observed after release of caged calcium (Beutner et al., 2001). Cell-attached capacitance recordings from posterior pituitary nerve terminals have resolved fusion of individual microvesicles, and about 5% of these events were followed by rapid reversal indicative of kiss-and-run (Klyachko and Jackson, 2002).

This overview indicates that the dominant mode of endocytosis at most synapses occurs with a time constant of 10–20 s. We have now shown that vesicle retrieval in hippocampal synapses occurs at a similar rate, and we identify this process as CME. Currently, the clearest evidence for a fast mechanism of vesicle retrieval occurs at the ribbon synapse of bipolar cells, where collapsed membrane is retrieved in 1 s by a process that is independent of clathrin (Llobet et al., 2003; Jockusch et al., 2005). It appears that fast endocytosis has greater functional importance at ribbon synapses that support continuous exocytosis in response to graded voltage signals compared with "classical" synapses that release vesicles in brief pulses triggered by action potentials.

Experimental Procedures

All experimental procedures are described in greater detail in the Supplemental Data.

Cell Culture

Primary cultures of rat hippocampal neurons were prepared from E18 rats and cocultured with glia. Neurons were transfected after 8 days in vitro (DIV) using lipofectamine2000 (Invitrogen) in MEM. Imaging experiments were then carried out at 14–21 DIV. For experiments in which CME was targeted using RNAi or mRFP-AP180-C,

transfections were carried out at 11 DIV and neurons imaged at 14 DIV. Immunocytochemistry, transferrin uptake, and quantification of CHC immunoreactivity or transferrin uptake in neurons was carried out as described previously (Royle et al., 2005).

Molecular Biology

SypHy was made in two steps. First, rat synaptophysin1 cDNA (NM_012664) was amplified by PCR from the ATG to behind the third TM region, introducing a GCCACC Kozak region before the ATG and XhoI and AgeI sites at the 5′ and 3′ ends, respectively. The product was then inserted into the synaptopHluorin vector via XhoI and AgeI, thereby connecting it to pHluorin and replacing the synaptobrevin region of synaptopHluorin. Second, to restore the fourth TM region and the C terminus of synaptophysin to sypHy, we used PCR to introduce AgeI sites at the 5′ and 3′ ends for insertion into the previous plasmid (before the stop codon) at AgeI. Full details of all DNA constructs used in this study are given in the Supplemental Data. CHC and scrambled siRNA were as previously described (Royle et al., 2005).

Live Imaging

Cells were perfused at ~0.2 ml/min with normal extracellular solution (comprised, in mM, of 136 NaCl, 2.5 KCl, 10 HEPES, 1.3 $MgCl_2$, 10 glucose, 2 $CaCl_2$, 0.01 CNQX, and 0.05 DL-APV [pH 7.4]) at 23°C ± 2°C. Fluorescence imaging was carried out on a Nikon Diaphot 200 microscope with a 40× (1.3 NA) oil immersion objective and a Xenon 100 W lamp. The filter set for pHluorin comprised a 475AF40 excitation filter, 505DRLP dichroic mirror, and a 535AF45 emission filter (Omega Filters). For mRFP constructs, the filter set comprised a 560AF55 excitation filter, 595DRLP dichroic mirror, and a 645AF75 emission filter. Illumination was shuttered only for time lapse experiments. Images were captured with a Photometrics Cascade 512B camera controlled by IPLab (Scanalytics). Electrical field stimulation was delivered via two parallel platinum wires 5 mm apart. A single AP was evoked by a 20 mA pulse of current lasting 1 ms.

For extracellular buffer exchange experiments, time lapse images of 512 × 512 pixels (binned 2 × 2) were acquired at 2 Hz with 195 ms exposure with a neutral density filter transmitting 25% of the illuminating light. The field of view was superfused with a gravity-fed laminar flow of buffer through a single barrel glass microelectrode fitted with two MicroFil (WPI) needles. The superfusing buffer was switched between HEPES buffer (pH 7.4) and MES buffer (pH 5.25) using solenoid valves (Lee Products Ltd.). Single AP stimulation was time-locked to frame acquisition and buffer changes.

For experiments monitoring pHluorin responses to single APs, images of 128 × 128 pixels (binned 2 × 2) were acquired at 5 Hz with 195 ms of exposure at full illumination. For each coverslip we acquired two data sets, the first one consisting of 10 APs at 45 s intervals (2325 images in total), the second consisting of the same 10 APs followed by a final train of 40 APs at 20 Hz (3000 images in total). To avoid bleaching pHluorin, transfected cells were first located using cotransfected mRFP.

For experiments investigating the effects of interfering with CME, time lapse images of sypHy (512 × 512 pixels) were acquired at 0.5 Hz with 250 ms of exposure at 25% illumination. Four or forty APs were delivered at 20 Hz. For experiments monitoring the movement of clathrin, synaptobrevin, and synaptophysin, two sets of time lapse images (150 images each, 512 × 512 pixels) were acquired at 0.5 Hz with 250 ms of exposure at 25% illumination. The stimulus protocol comprised 4, 40, and 400 APs delivered at 20 Hz after 40, 100, and 160 s. The first data set was taken with the mRFP filter set and the second (sypHy) data set was taken after 5 min.

Image Analysis

Images were analyzed using custom-written macros in IPLab and Igor Pro software. Responding synapses were identified using "difference images" highlighting the stimulus-dependent increase in sypHy fluorescence. These difference images were constructed by subtracting a five-frame average obtained immediately before a test train of 20 or 40 APs from a five-frame average obtained just after stimulation. Square ROIs were then positioned at the center of exocytic hotspots, revealing active synapses. The standard ROI size was 1.6 × 1.6 μm and the precise location was selected to maximize the basal fluorescence within the ROI before stimulation. Larger ROIs (4.8 × 4.8 μm) and perimeter zones (outer width of 4.8 μm and depth of 0.8 μm) were then positioned to encompass smaller ROIs within their centers. In buffer exchange experiments, ROIs were 2.4 × 2.4 μm.

Experiments in which CME was targeted were analyzed using ROIs positioned over synapses using the method described above. An ROI of 1.6 × 1.6 μm was used to quantify responses to four APs and the larger ROI of 4.8 × 4.8 μm for responses to 40 APs. In experiments monitoring the diffusion of clathrin, synaptobrevin, and synaptophysin, synapses were first identified in the sypHy movie clip as described above. ROIs of 1.2 × 1.2 μm were centered over synapses, and then transferred to the mRFP movie clip. Measurements at each synapse were normalized before averaging and then corrected for bleach.

Supplemental Data

The Supplemental Data for this article can be found online at http://www.neuron.org/cgi/content/full/51/6/773/DC1/.

Acknowledgments

The authors would like to thank Jim Rothman, Ernst Ungewickel, and Harvey McMahon for kind gifts of plasmids. We are indebted to Aude Derevier for preparation of hippocampal cultures. This work was supported by the Swedish Research Council (B.G.) and HFSP (L.L.).

Received: February 21, 2006
Revised: August 3, 2006
Accepted: August 28, 2006
Published: September 20, 2006

References

Aravanis, A.M., Pyle, J.L., Harata, N.C., and Tsien, R.W. (2003a). Imaging single synaptic vesicles undergoing repeated fusion events: kissing, running, and kissing again. Neuropharmacology *45*, 797–813.

Aravanis, A.M., Pyle, J.L., and Tsien, R.W. (2003b). Single synaptic vesicles fusing transiently and successively without loss of identity. Nature *423*, 643–647.

Atluri, P.P., and Ryan, T.T. (2006). The kinetics of synaptic vesicle reacidification at hippocampal nerve terminals. J. Neurosci. *26*, 2313–2320.

Auger, C., and Marty, A. (2000). Quantal currents at single-site central synapses. J. Physiol. *526*, 3–11.

Bekkers, J.M. (1994). Quantal analysis of synaptic transmission in the central nervous system. Curr. Opin. Neurobiol. *4*, 360–365.

Bekkers, J.M., and Stevens, C.F. (1995). Quantal analysis of EPSCs recorded from small numbers of synapses in hippocampal cultures. J. Neurophysiol. *73*, 1145–1156.

Beutner, D., Voets, T., Neher, E., and Moser, T. (2001). Calcium dependence of exocytosis and endocytosis at the cochlear inner hair cell afferent synapse. Neuron *29*, 681–690.

Biro, A.A., Holderith, N.B., and Nusser, Z. (2005). Quantal size is independent of the release probability at hippocampal excitatory synapses. J. Neurosci. *25*, 223–232.

Bruns, D., Riedel, D., Klingauf, J., and Jahn, R. (2000). Quantal release of serotonin. Neuron *28*, 205–220.

Dickman, D.K., Horne, J.A., Meinertzhagen, I.A., and Schwarz, T.L. (2005). A slowed classical pathway rather than kiss-and-run mediates endocytosis at synapses lacking synaptojanin and endophilin. Cell *123*, 521–533.

Dobrunz, L.E., and Stevens, C.F. (1997). Heterogeneity of release probability, facilitation, and depletion at central synapses. Neuron *18*, 995–1008.

Fernandez-Alfonso, T., Kwan, R., and Ryan, T.A. (2006). Synaptic vesicles interchange their membrane proteins with a large surface reservoir during recycling. Neuron *51*, 179–186.

Fesce, R., Grohovaz, F., Valtorta, F., and Meldolesi, J. (1994). Neurotransmitter release: fusion or 'kiss-and-run'? Trends Cell Biol. *4*, 1–4.

Ford, M.G., Pearse, B.M., Higgins, M.K., Vallis, Y., Owen, D.J., Gibson, A., Hopkins, C.R., Evans, P.R., and McMahon, H.T. (2001). Simultaneous binding of PtdIns(4,5)P2 and clathrin by AP180 in the nucleation of clathrin lattices on membranes. Science *291*, 1051–1055.

Franks, K.M., Stevens, C.F., and Sejnowski, T.J. (2003). Independent sources of quantal variability at single glutamatergic synapses. J. Neurosci. *23*, 3186–3195.

Frerking, M., Schulte, J., Wiebe, S.P., and Staubli, U. (2005). Spike timing in CA3 pyramidal cells during behavior: implications for synaptic transmission. J. Neurophysiol. *94*, 1528–1540.

Gandhi, S.P., and Stevens, C.F. (2003). Three modes of synaptic vesicular recycling revealed by single-vesicle imaging. Nature *423*, 607–613.

Hallermann, S., Pawlu, C., Jonas, P., and Heckmann, M. (2003). A large pool of releasable vesicles in a cortical glutamatergic synapse. Proc. Natl. Acad. Sci. USA *100*, 8975–8980.

Harata, N., Ryan, T.A., Smith, S.J., Buchanan, J., and Tsien, R.W. (2001). Visualizing recycling synaptic vesicles in hippocampal neurons by FM 1-43 photoconversion. Proc. Natl. Acad. Sci. USA *98*, 12748–12753.

Harata, N.C., Choi, S., Pyle, J.L., Aravanis, A.M., and Tsien, R.W. (2006). Frequency-dependent kinetics and prevalence of kiss-and-run and reuse at hippocampal synapses studied with novel quenching methods. Neuron *49*, 243–256.

Heidelberger, R., Zhou, Z.Y., and Matthews, G. (2002). Multiple components of membrane retrieval in synaptic terminals revealed by changes in hydrostatic pressure. J. Neurophysiol. *88*, 2509–2517.

Heuser, J.E., and Reese, T.S. (1973). Evidence for recycling of synaptic vesicle membrane during transmitter release at the frog neuromuscular junction. J. Cell Biol. *57*, 315–344.

Holt, M., Cooke, A., Neef, A., and Lagnado, L. (2004). High mobility of vesicles supports continuous exocytosis at a ribbon synapse. Curr. Biol. *14*, 173–183.

Hull, C., and von Gersdorff, H. (2004). Fast endocytosis is inhibited by GABA-mediated chloride influx at a presynaptic terminal. Neuron *44*, 469–482.

Jockusch, W.J., Praefcke, G.J., McMahon, H.T., and Lagnado, L. (2005). Clathrin-dependent and clathrin-independent retrieval of synaptic vesicles in retinal bipolar cells. Neuron *46*, 869–878.

Katz, B. (1969). The Release of Neural Transmitter Substances (Liverpool, England: Liverpool University Press).

Klingauf, J., Kavalali, E.T., and Tsien, R.W. (1998). Kinetics and regulation of fast endocytosis at hippocampal synapses. Nature *394*, 581–585.

Klyachko, V.A., and Jackson, M.B. (2002). Capacitance steps and fusion pores of small and large-dense-core vesicles in nerve terminals. Nature *418*, 89–92.

Li, Z., and Murthy, V.N. (2001). Visualizing postendocytic traffic of synaptic vesicles at hippocampal synapses. Neuron *31*, 593–605.

Li, Z., Burrone, J., Tyler, W.J., Hartman, K.N., Albeanu, D.F., and Murthy, V.N. (2005). Synaptic vesicle recycling studied in transgenic mice expressing synaptopHluorin. Proc. Natl. Acad. Sci. USA *102*, 6131–6136.

Llobet, A., Beaumont, V., and Lagnado, L. (2003). Real-time measurement of exocytosis and endocytosis at synapses and neuroendocrine cells using interference reflection microscopy. Neuron *40*, 1075–1086.

Marte, B. (2002). An encore for kiss and run? Nat. Cell Biol. *4*, E123.

Merrifield, C.J., Perrais, D., and Zenisek, D. (2005). Coupling between clathrin-coated-pit invagination, cortactin recruitment, and membrane scission observed in live cells. Cell *121*, 593–606.

Miesenbock, G., De Angelis, D.A., and Rothman, J.E. (1998). Visualizing secretion and synaptic transmission with pH-sensitive green fluorescent proteins. Nature *394*, 192–195.

Motley, A., Bright, N.A., Seaman, M.N., and Robinson, M.S. (2003). Clathrin-mediated endocytosis in AP-2-depleted cells. J. Cell Biol. *162*, 909–918.

Mueller, V.J., Wienisch, M., Nehring, R.B., and Klingauf, J. (2004). Monitoring clathrin-mediated endocytosis during synaptic activity. J. Neurosci. *24*, 2004–2012.

Mundigl, O., Ochoa, G.C., David, C., Slepnev, V.I., Kabanov, A., and De Camilli, P. (1998). Amphiphysin I antisense oligonucleotides inhibit neurite outgrowth in cultured hippocampal neurons. J. Neurosci. *18*, 93–103.

Murthy, V.N., Sejnowski, T.J., and Stevens, C.F. (1997). Heterogeneous release properties of visualized individual hippocampal synapses. Neuron *18*, 599–612.

Neves, G., and Lagnado, L. (1999). The kinetics of exocytosis and endocytosis in the synaptic terminal of goldfish retinal bipolar cells. J. Physiol. *515*, 181–202.

Pyle, J.L., Kavalali, E.T., Piedras-Renteria, E.S., and Tsien, R.W. (2000). Rapid reuse of readily releasable pool vesicles at hippocampal synapses. Neuron *28*, 221–231.

Richards, D.A., Bai, J., and Chapman, E.R. (2005). Two modes of exocytosis at hippocampal synapses revealed by rate of FM1-43 efflux from individual vesicles. J. Cell Biol. *168*, 929–939.

Ringstad, N., Gad, H., Low, P., Di Paolo, G., Brodin, L., Shupliakov, O., and De Camilli, P. (1999). Endophilin/SH3p4 is required for the transition from early to late stages in clathrin-mediated synaptic vesicle endocytosis. Neuron *24*, 143–154.

Rizzoli, S.O., and Betz, W.J. (2003). Neurobiology: All change at the synapse. Nature *423*, 591–592.

Rizzoli, S.O., and Betz, W.J. (2005). Synaptic vesicle pools. Nat. Rev. Neurosci. *6*, 57–69.

Rosenmund, C., and Stevens, C.F. (1996). Definition of the readily releasable pool of vesicles at hippocampal synapses. Neuron *16*, 1197–1207.

Royle, S.J., and Lagnado, L. (2003). Endocytosis at the synaptic terminal. J. Physiol. *553*, 345–355.

Royle, S.J., Bright, N.A., and Lagnado, L. (2005). Clathrin is required for the function of the mitotic spindle. Nature *434*, 1152–1157.

Sankaranarayanan, S., and Ryan, T.A. (2000). Real-time measurements of vesicle-SNARE recycling in synapses of the central nervous system. Nat. Cell Biol. *2*, 197–204.

Sankaranarayanan, S., and Ryan, T.A. (2001). Calcium accelerates endocytosis of vSNAREs at hippocampal synapses. Nat. Neurosci. *4*, 129–136.

Schikorski, T., and Stevens, C.F. (2001). Morphological correlates of functionally defined synaptic vesicle populations. Nat. Neurosci. *4*, 391–395.

Stiles, J.R., Van Helden, D., Bartol, T.M., Jr., Salpeter, E.E., and Salpeter, M.M. (1996). Miniature endplate current rise times less than 100 microseconds from improved dual recordings can be modeled with passive acetylcholine diffusion from a synaptic vesicle. Proc. Natl. Acad. Sci. USA *93*, 5747–5752.

Sun, J.Y., Wu, X.S., and Wu, L.G. (2002). Single and multiple vesicle fusion induce different rates of endocytosis at a central synapse. Nature *417*, 555–559.

Takei, K., Mundigl, O., Daniell, L., and De Camilli, P. (1996). The synaptic vesicle cycle: a single vesicle budding step involving clathrin and dynamin. J. Cell Biol. *133*, 1237–1250.

Tyler, W.J., and Murthy, V.N. (2004). Synaptic vesicles. Curr. Biol. *14*, R294–R297.

Valtorta, F., Pennuto, M., Bonanomi, D., and Benfenati, F. (2004). Synaptophysin: leading actor or walk-on role in synaptic vesicle exocytosis? Bioessays *26*, 445–453.

van Santen, R.A., and Niemantsverdiet, J.W. (1995). Chemical Kinetics and Catalysis (New York: Plenum).

Verstreken, P., Kjaerulff, O., Lloyd, T.E., Atkinson, R., Zhou, Y., Meinertzhagen, I.A., and Bellen, H.J. (2002). Endophilin mutations block clathrin-mediated endocytosis but not neurotransmitter release. Cell *109*, 101–112.

Wienisch, M., and Klingauf, J. (2006). Vesicular proteins exocytosed and subsequently retrieved by compensatory endocytosis are nonidentical. Nat. Neurosci. *9*, 1019–1027.

Yamashita, T., Hige, T., and Takahashi, T. (2005). Vesicle endocytosis requires dynamin-dependent GTP hydrolysis at a fast CNS synapse. Science *307*, 124–127.

Yao, P.J., Zhang, P., Mattson, M.P., and Furukawa, K. (2003). Heterogeneity of endocytic proteins: distribution of clathrin adaptor proteins in neurons and glia. Neuroscience *121*, 25–37.

Zenisek, D., Steyer, J.A., Feldman, M.E., and Almers, W. (2002). A membrane marker leaves synaptic vesicles in milliseconds after exocytosis in retinal bipolar cells. Neuron *35*, 1085–1097.